Laser and Particle Beams (2000), *18*, 563–570. Printed in the USA.

Generation, characterization, and medical utilization of laser-produced emission continua

S. SVANBERG,[1] S. ANDERSSON-ENGELS,[1] R. CUBEDDU,[2] E. FÖRSTER,[3] M. GRÄTZ,[1]
K. HERRLIN,[1] G. HÖLZER,[3] L. KIERNAN,[1] C. AF KLINTEBERG,[1] A. PERSSON,[1]
A. PIFFERI,[2] A. SJÖGREN,[1] AND C.-G. WAHLSTRÖM[1]

[1]Lund Laser Centre, P.O. Box 118, S-221 00 Lund, Sweden
[2]Politecnico di Milano, Piazza Leonardo da Vinci 32, I-20133 Milano, Italy
[3]Friedrich Schiller Universität, Max-Wien-Platz 1, D-07743 Jena, Germany

(RECEIVED 22 July 1999; ACCEPTED 20 September 1999)

Abstract

Intense continua of electromagnetic radiation of very brief duration are formed in the interaction of focused ultra-short terawatt laser pulses with matter. Two different kinds of experiments, which have been performed utilizing the Lund 10 Hz titanium-doped sapphire terawatt laser system are being described, where visible radiation and X-rays, respectively, have been generated. Focusing into water leads to the generation of a light continuum through self-phase modulation. The propagation of the light through tissue was studied addressing questions related to optical mammography and specific chromophore absorption. When terawatt laser pulses are focused onto a solid target with high nuclear charge *Z*, intense X-ray radiation of few ps duration and with energies exceeding hundreds of keV is emitted. Biomedical applications of this radiation are described, including differential absorption and gated-viewing imaging.

1. INTRODUCTION

Very soon after the invention of the laser, medical applications started to emerge. Initially, the thermal effects of the radiation were utilized. The techniques have been refined and the laser is now routinely used for treatment in many specialities including ophthalmology and surgery. Diagnostic use of laser radiation came later. During the last 15 years laser spectroscopic techniques have been developed providing powerful means for nonintrusive medical diagnostics of tissue in real time (see, e.g., Svanberg, 1997; Svanberg, 1999). The field includes the early diagnostics and demarcation of malignant tumors, the characterization of blood vessels for guiding interventional angioplastic procedures, and scattering spectroscopy for optical mammography, etc. Laser-induced chemistry (photodynamic therapy) can also be applied for the eradication of tumors (see, e.g., Svanberg *et al.*, 1994*a*; Wang *et al.*, 1999). Lasers for medical applications are generally reasonably compact. In the present paper we will discuss the use of large laser systems in biomedical research. We have used a terawatt laser system to generate intense continua of electromagnetic radiation and have studied the propagation of the radiation through tissue aiming at the development of novel medical imaging techniques. Ultrashort bursts of white light or X-rays were achieved in the interaction between the ultra-intense laser pulses with matter, and wavelength dispersive and time-resolving detection systems were used to follow the subsequent interaction with tissue. The aim of the experiments is to study fundamental interactions and to provide an understanding of possibilities and limitations of the techniques, enabling the evaluation of the possibility of achieving clinically adaptable systems.

2. LUND HIGH-POWER CHIRPED-PULSE AMPLIFICATION SYSTEM

A multi-terawatt chirped-pulse amplification laser system based on titanium-doped sapphire is being operated at the Lund high-power laser facility, which was established in 1992 (Svanberg *et al.*, 1994*b*). It is the spearhead in a park of high-power laser systems with different and complementary characteristics. The large system has been continuously upgraded, and the present layout is shown in Figure 1. The system is based on chirped pulse amplification (CPA) which is a new technique to achieve extremely high optical intensities in compact laser systems. An initial, short pulse is tem-

Address correspondence and reprint requests to: S. Svanberg, Department of Physics, Lund Institute of Technology, P.O. Box 118, S-221 00 Lund, Sweden. E-mail: sune.svanberg@fysik.lth.se

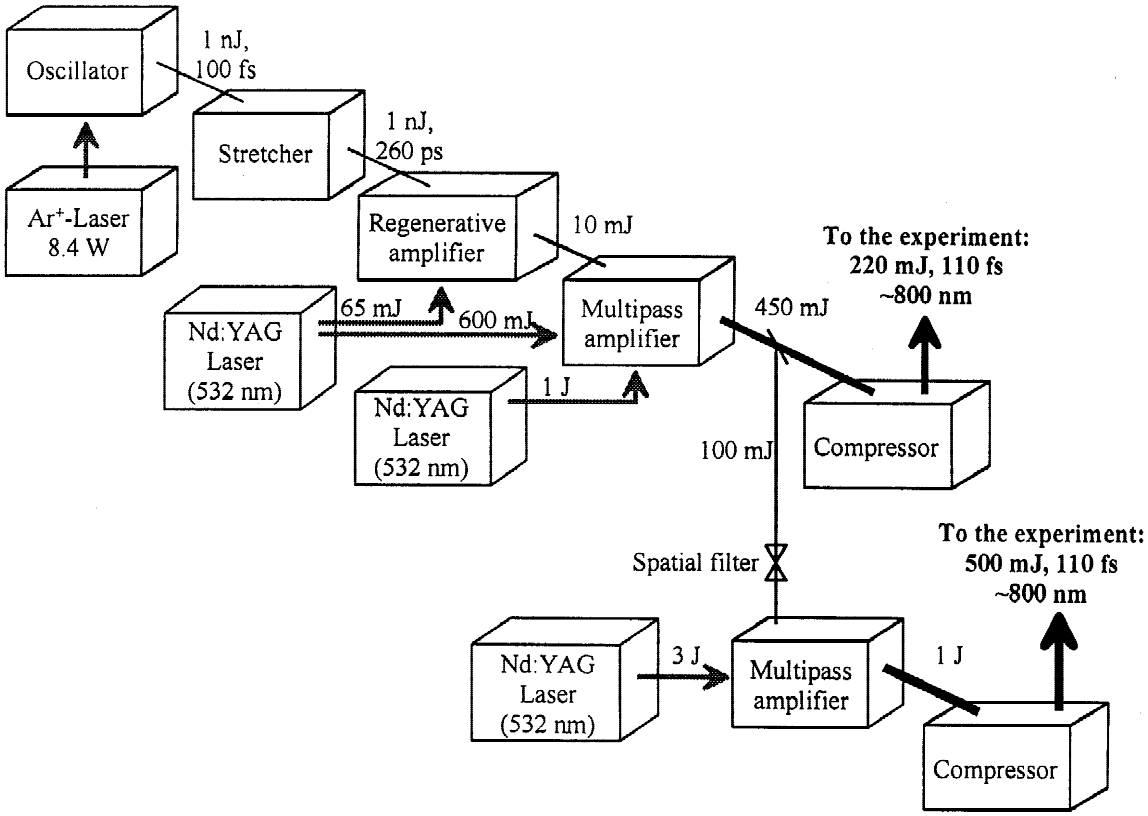

Fig. 1. Layout of the Lund chirped-pulse amplification terawatt laser system (from Grätz, 1998).

porally stretched before amplification in order to reduce the peak power in the amplifier stage for a given pulse energy, avoiding the need for large beam diameters. Pulse compression is then performed in a grating arrangement to achieve ultra-high powers. Through the introduction of titanium-doped sapphire (Ti:S) as a gain medium, particularly convenient systems can be accomplished. Ti:S can readily be pumped by Nd:YAG radiation that is frequency doubled to 532 nm. The material has a wide gain profile and can thus support amplification of ultrashort pulses (down to tens of fs), which results in lower pulse-energy demands for reaching terawatt power levels at a repetition rate of 10 Hz. Important quality factors describing a terawatt laser are, apart from the pulse power, the pulse duration, the focusability and the contrast between the main pulse and possible prepulses or a background level (pedestal).

Nearly transform-limited pulses of 100 fs duration are generated from an Ar^+-laser pumped Kerr-lens mode locked Ti:S oscillator (Coherent Mira 900). Pulses at a repetition rate of 76 MHz and at an average power of about 1 W (10 nJ/pulse, 100 kW peak power) are obtained. The 100 fs pulsewidth is determined by remaining, noncompensated group-velocity dispersion in the oscillator cavity and can be further reduced. The 100 fs output pulses from the oscillator are temporally stretched by a factor of about 2500 in a grating and lens arrangement that is double-passed. The stretched oscillator pulse is injected into a regenerative Ti:S amplifier (polarization switching using an intracavity Pockels cell and thin-film polarizers). This unit is basically a Ti:S laser which is pumped by 65 mJ of green light from a frequency doubled Nd:YAG laser. After 14 double passes and about 10^6 times amplification, the pulse is ejected, again by polarization switching. A further Pockels cell is used to suppress any cavity leakage of other pulses than the main one. Power boosting is performed in a six-pass (butterfly) Ti:S amplifier crystal to reach a level of up to 450 mJ. Two frequency-doubled high-energy Nd:YAG lasers pump the amplifier at a total energy level of 1.6 J at 10 Hz. Relay imaging of the pump laser-rod surface using evacuated beam-transport telescopes is used to achieve a more uniform pumping. A beam diameter of 8 mm is used through the final Ti:S crystal. About 350 mJ of this radiation is used for an intermediate power outlet. The beam is expanded to 50 mm diameter, in order to reduce the power density, the pulse is compressed using two parallel, 11×11 cm gold-coated holographic gratings with 1800 grooves/mm and a first-order diffraction efficiency of about 90%. After double passing the grating arrangement the low-frequency leading-edge light is delayed and the high-frequency trailing edge is catching up to emerge simultaneously from the compressor. 110 fs pulses of powers up to 2 TW can be obtained around 790 nm. 100 mJ of the primary beam is split off and passed through a vacuum spatial filter and is injected into a high-power 4 pass amplifier which is pumped by about 3 J of green output pulses from a further

https://doi.org/10.1017/S0263034600183302 Published online by Cambridge University Press

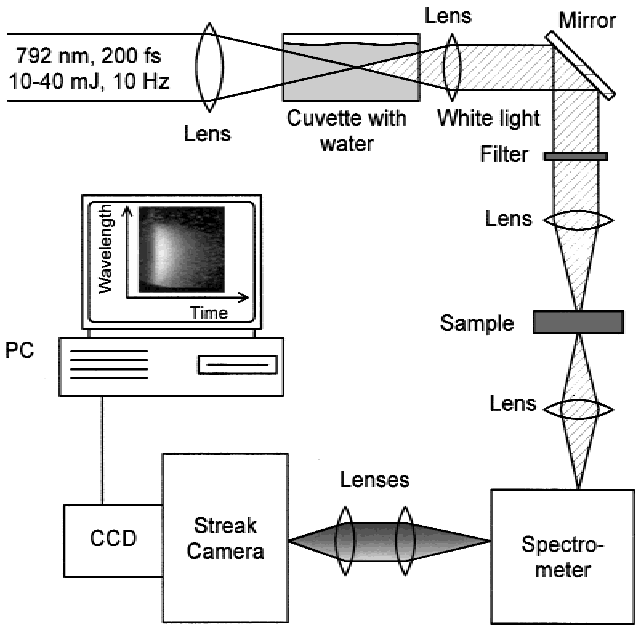

Fig. 2. Setup for time-resolved photon propagation studies using white light (from Andersson-Engels *et al.*, 1993).

high-energy Nd:YAG system. About 1J of energy is achieved in the amplifier. The beam is expanded and passed into a separated vacuum tank compressor with similar gratings as in the already discussed compressor. More than 4 TW is achieved in 110 fs pulses. The system will now be upgraded to 8 TW and later; mainly by shortening the pulse to 50 fs, be upgraded to 20 TW.

3. WHITE LIGHT GENERATION AND APPLICATIONS

When high-power laser pulses are focused into water a light continuum is generated through self-phase modulation. The origin of the phenomenon is the dependence of the index of refraction on the light intensity, leading to frequency chirps when the pulse is rising and falling. Following the injection of such pulses into strongly scattering media, such as tissue, the time dispersion of the photons can be studied. The spectral contents and the time duration of the radiation can be measured with a streak camera coupled to the exit slit of a spectrometer. A 2D representation of time *versus* color is obtained. An experimental set-up for studies of this kind is shown in Figure 2. An example of a spectral distribution of the generated light is shown in Figure 3. The experiments allowed the study of transillumination dynamics through tissue at all visible wavelengths simultaneously (Andersson-Engels *et al.*, 1993), facilitating feasibility studies and optimum wavelength choice for optical mammography (Berg *et al.*, 1993). An example of a 2D recording is shown in Figure 4. More recently, we have extended these type of measurements to the study of absorption spectra of sensitizers *in situ* in living tissue (af Klinteberg *et al.*, 1999). A rat tumor model was used, where a human adenocarcinoma, inoculated on the hind leg muscle produced tumors of about

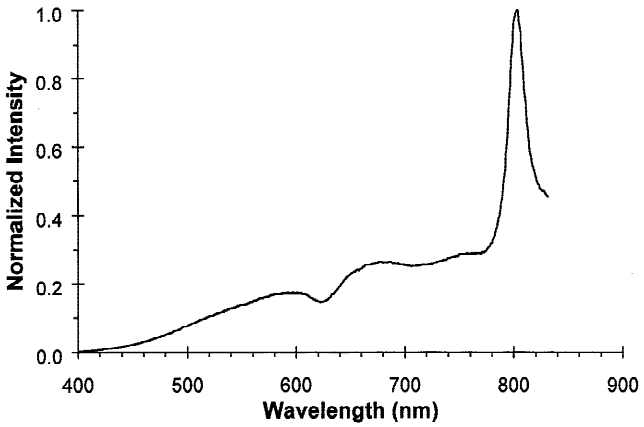

Fig. 3. Typical spectral distribution of "white light" generated by self-phase-modulation of femtosecond titanium-sapphire pulses in water (from af Klinteberg *et al.*, 1999).

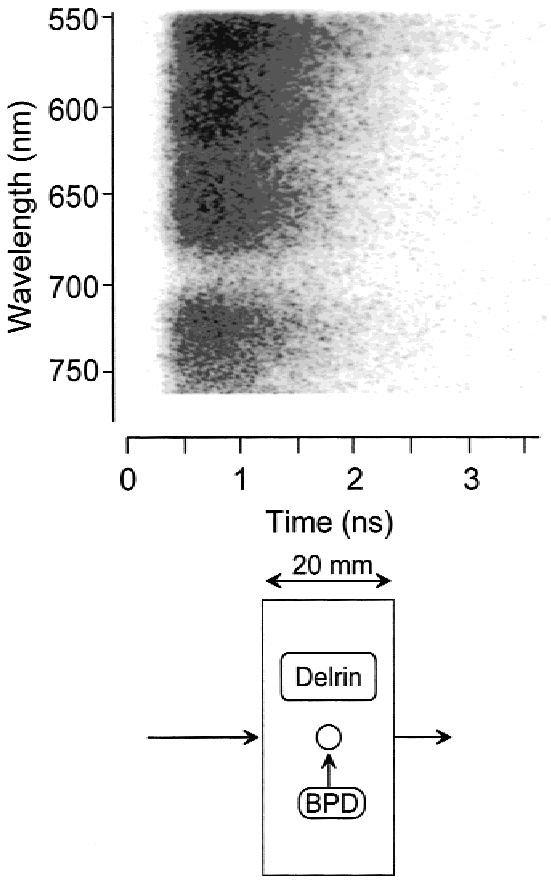

Fig. 4. 2D representation of experimental data on a Delrin sample of scattering plastic containing a cavity filled with the tumor sensitizing agent bensoporphyrine derivative (Quadralogics, Vancouver). The photon temporal dispersion as a function of the wavelength is shown with the absorption band of the bensoporphyrin molecules clearly visible.

https://doi.org/10.1017/S0263034600183302 Published online by Cambridge University Press

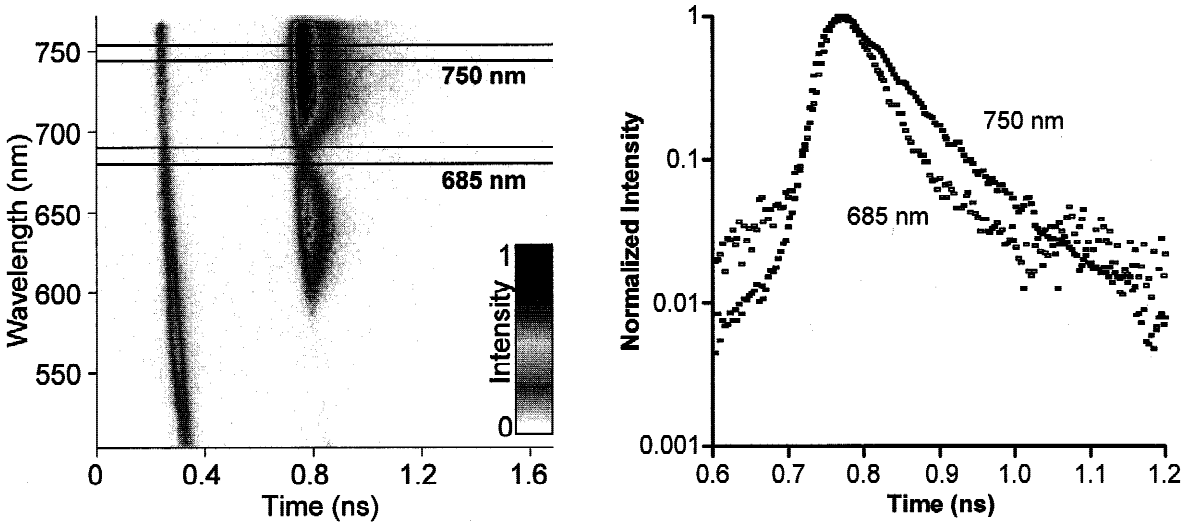

Fig. 5. 2D recording of white-light photons diffusely scattered through rat tissue loaded with disulphonated aluminium phtalocyanine. Transmission and receiving fibers were separated by 8 mm. Dispersion curves taken for two narrow wavelength regions, on and off the sensitizer absorption are shown, featuring different behaviors (from af Klinteberg *et al.*, 1999).

15 mm diameter. Optical fibers were used to inject the light in the tissue and to collect scattered light emerging again at a distance of about 8 mm. The rats were injected with disulphonated aluminum phtalocyanine at a concentration of 2.5 or 5 mg/kg body weight and measurements were performed both on tumor and normal tissue. A recording is shown in Figure 5, where also temporal dispersion curves are displayed for two wavelengths. From such curves the absorption and scattering coefficients can be extracted using the method discussed by Cubeddu *et al.*, (1996). This allows the plotting of the absorption profile of the sensitizer *in vivo* (Fig. 6), showing a wavelength redshift with regard to a water solution. A tumor/normal tissue uptake true ratio of about 2 can also be inferred. Similar techniques can be used to extract tissue absorption and scattering properties related to optical mammography (af Klinteberg *et al.*, 1995). Studies on other scattering media, such as plant leaves (Johansson *et al.*, 1999) have also been performed.

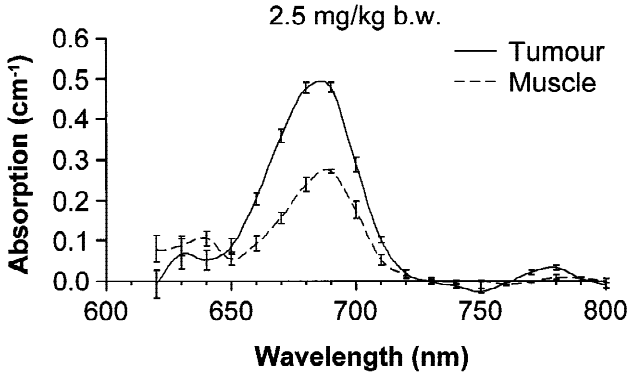

Fig. 6. Plots of the absorption curves for phtalocyanine, recorded for the tumor and for normal surrounding tissue (from af Klinteberg *et al.*, 1999).

4. X-RAY GENERATION AND APPLICATIONS

When terawatt laser pulses are focused onto a solid target with high nuclear charge *Z*, intense X-ray radiation of few ps duration and with energies exceeding hundreds of keV is emitted (Kmetec *et al.*, 1992; Herrlin *et al.*, 1993). A general layout for that type of experiment is shown in Figure 7. The spectral content of the radiation was studied by energy dispersive techniques (Tillman *et al.*, 1997), where pile-up problems due to the burst nature of the radiation have to be properly addressed, and by crystal spectroscopy using Bragg and Laue geometry (Hölzer *et al.*, 1997; Hölzer *et al.*, 1999). A spectral recording for tantalum using the Bragg geometry is given in Figure 8. It was shown, that some 2×10^8 photons were obtained in the *K*-α lines of tantalum around 57 keV. Ultrasharp and single-shot imaging was achieved in our early work (Herrlin *et al.*, 1993; Tillman *et al.*, 1995). Imaging of small animals could be achieved as demonstrated in Figure 9. Feasibility experiments utilizing differential absorption across a *K* absorption edge have been performed (Tillman *et al.*, 1996). Here, the *K* lines of tantalum and gadolinium targets were used to bridge the 50 keV *K*-absorption edge of gadolinium used as a contrast agent. Figure 10 displays images for rats with Gd and Ce-based contrast agents, respectively, administered to their stomachs. Tantalum and gadolinium targets were used in the X-ray source. Since the *K*-α emission lines bridge the gadolinium absorption edge but not the cerium one, different behaviors are seen in the two animals.

Further, the short temporal duration of the laser-produced X-ray pulses has been utilized in time-gated viewing experiments (Gordon *et al.*, 1995; Grätz *et al.*, 1996) to suppress Compton-scattered photons, potentially allowing a dose reduction in medical X-ray imaging. Normally, such scattered radiation is suppressed employing antiscattering grids (tun-

https://doi.org/10.1017/S0263034600183302 Published online by Cambridge University Press

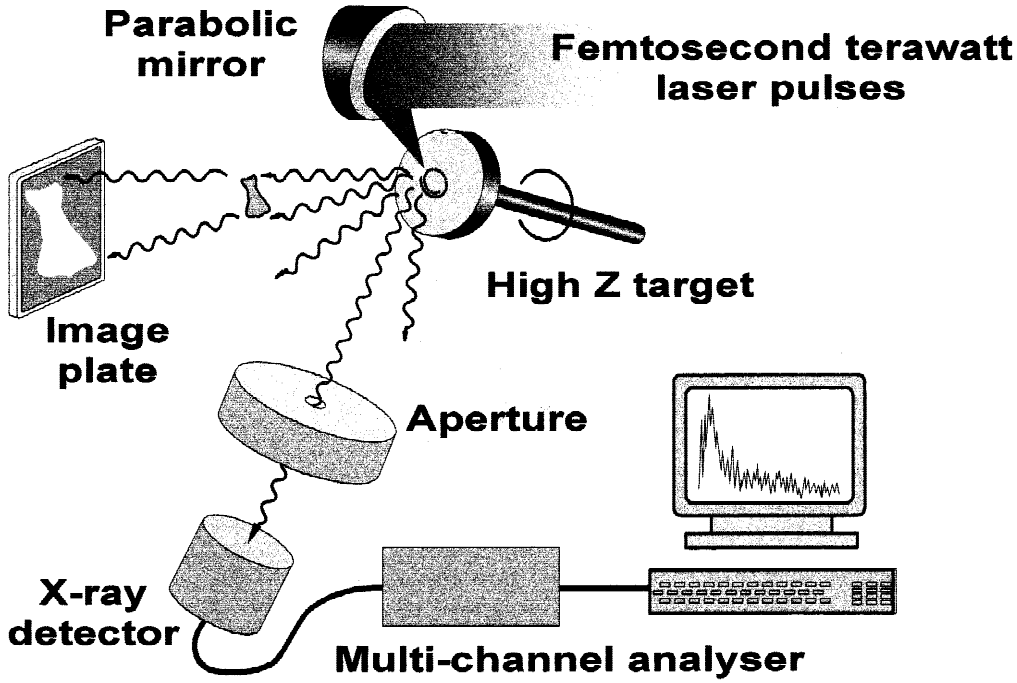

Fig. 7. Experimental setup for the production of hard X-ray radiation in the interaction of ultraintense laser pulses with a metal target (from Tillman, 1997).

nel vision), but this leads to an increased patient dose, since the grids also block out useful photons. We have performed extensive modeling and experimental work illustrating possibilities and limitations for time-gated X-ray viewing. Linear imaging using an X-ray streak camera is shown in Figure 11 simulating the cases of mammographic and whole-body applications. Without time resolution, a lead obstacle is shown with strongly reduced contrast due to the scattering. By restricting the imaging to the ballistic photons only, contrast is strongly enhanced. Recently, the gated-viewing concept has been combined with tomographic back-projection to yield scatter-reduced 2D images of tissue phantoms (Grätz *et al.*, 1998).

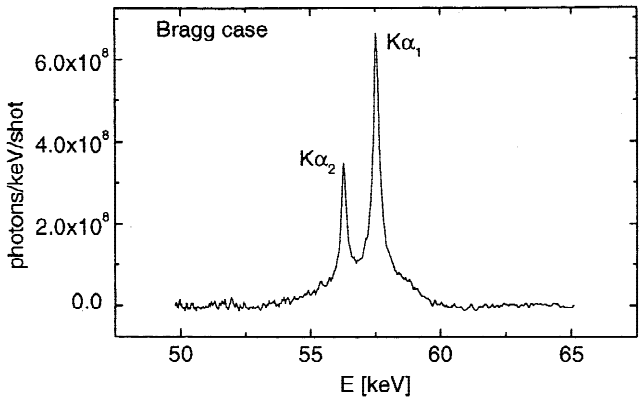

Fig. 8. X-ray spectrum for a tantalum target, recorded around the *K*-α lines using a crystal spectrometer with a scintillator/ccd detector arrangement (from Hölzer *et al.*, 1999).

Fig. 9. X-ray image of a sacrificed Wistar-Furth rat, recorded on a normal radiographic imaging plate using a thin copper filter to cut off most of the radiation with energy below 25 keV.

https://doi.org/10.1017/S0263034600183302 Published online by Cambridge University Press

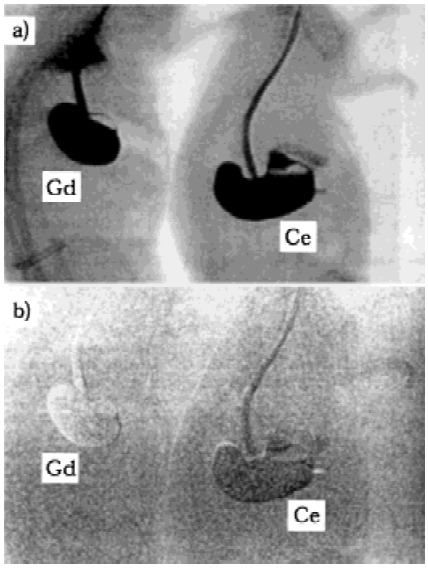

Fig. 10. Differential imaging of the stomach regions of two sacrificed Wistar-Furth rats (200 g) given gadolinium and cerium-containing contrast agents. The upper part of the figure shows direct recordings and the lower part the result of division of images taken for the gadolinium and the tantalum source (from Herrlin *et al.*, 1997).

5. DISCUSSION

The use of laser-produced continua of electromagnetic radiation in the visible and in the X-ray regions has been discussed in this paper. A large TW research laser system, operating at a repetition rate of 10 Hz was used in proof-of-principle experiments. In the white-light generation experiments only a fraction of the pulse energy was used. Actually, a new 1 kHz, 30 fs pulselength laser system, based on the CPA technology in titanium-doped sapphire, which recently became available at the Lund high-power laser facility is more suited for the purpose, because of the higher average power available, especially when a planned pulse-energy upgrade from 1.5 mJ/pulse to 5 and possibly 10 mJ/pulse has been completed. The white-light set-up has the virtue to allow simultaneous assessment of all relevant wavelengths in the study of absorptive and scattering properties of tissues and optical contrast agents. Based on the results, pulsed diode lasers at optimal wavelengths can be chosen for clinically adapted equipment.

Regarding the realism of a diagnostic system based on laser-produced X-rays, several aspects have to be considered. A basic question is of course, if the absorbed dose of X-rays delivered as intense spikes of ultrashort duration has the same biological effect as an equivalent dose of conventional, CW X-ray radiation. Initial experiments on survival rates for Chinese hamster cells show that this is indeed the case (See Fig. 12) (Tillman *et al.*, 1999); otherwise the concept would have to be abandoned at once. The generation of adequate amounts of radiation for human radiography needs a laser sysem with a higher repetition rate than the one employed; again, the 1 kHz short-pulse system mentioned above will provide possibilities to perform scaling-up experiments. Synchrotrons are already being used for differential absorption measurements for dose-reduction in angiography using an iodine contrast agent (Gmür *et al.*, 1995). To make the laser-based source advantageous over synchrotrons or conventional sources, some way to enhance the characteristic line emission over the bremsstrahlung continuum would have to be found. The greatest potential of the laser-based

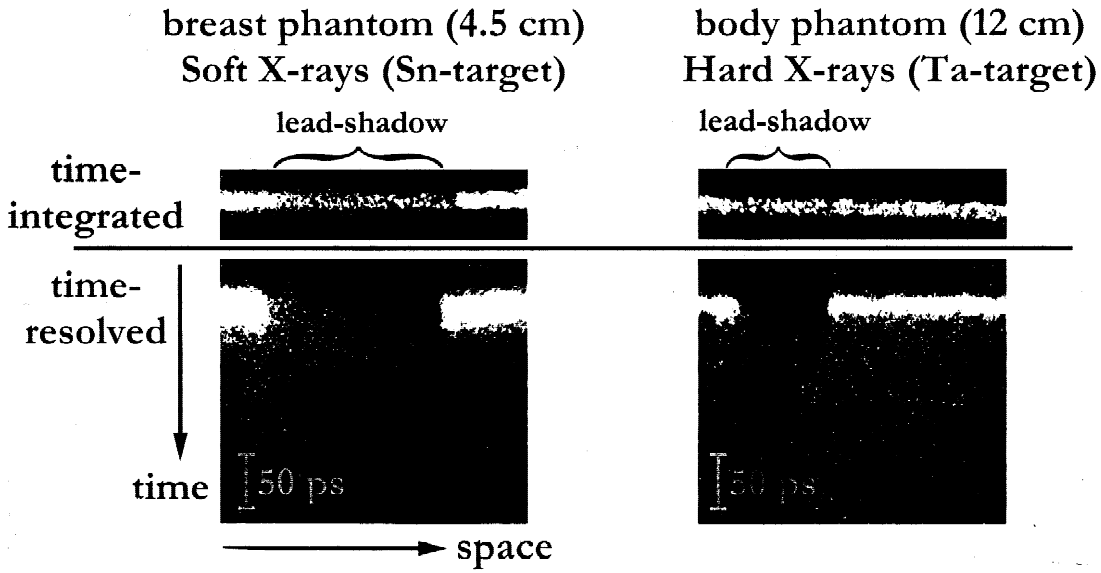

Fig. 11. 1D X-ray imaging of a blocking lead strip placed in front of water phantoms relevant for mammography and whole body transillumination imaging. The retrieval of contrast when only ballistic X-ray photons are employed is demonstrated (from Grätz *et al.*, 1996).

https://doi.org/10.1017/S0263034600183302 Published online by Cambridge University Press

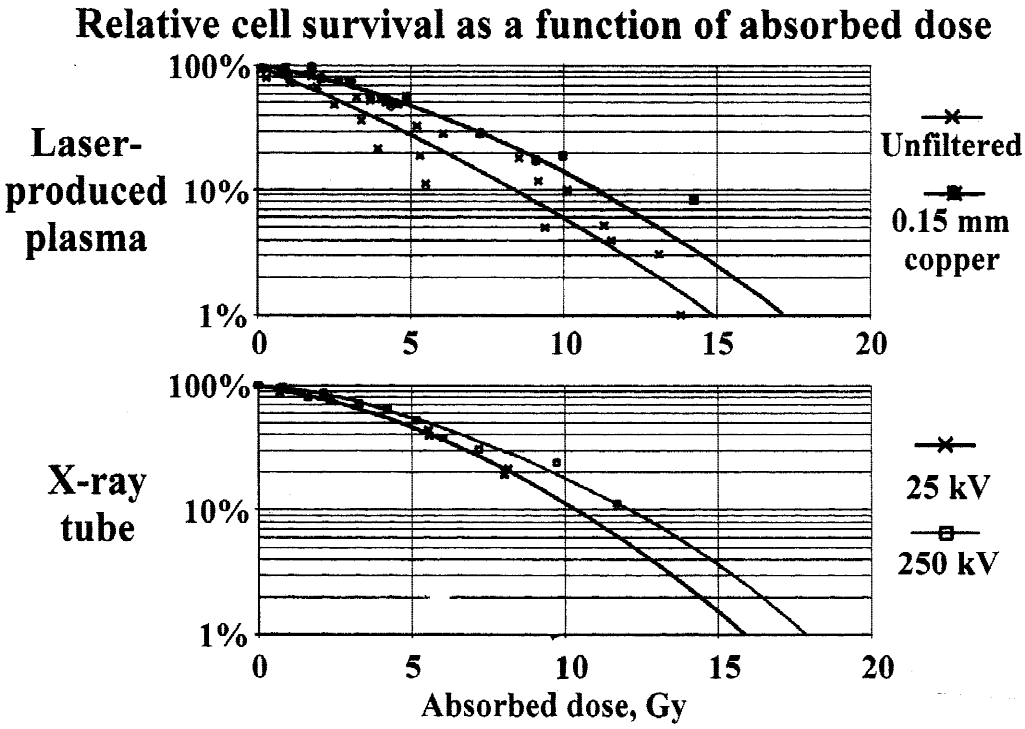

Fig. 12. Survival curves for V79-CH cells subject to laser-produced X-rays and conventional ionizing radiation from a 25 kV and a 250 kV conventional X-ray tube. The diagram shows that the radiation from the different sources has similar influence on live biological specimen (from Tillman *et al.*, 1999).

X-ray source seems to be for the gated-viewing reduction of Compton-scattered radiation, since even modest reductions in absorbed X-ray doses could mean substantial savings in radiation-damage induced suffering and costs. A high average power source would then have to be integrated with a high-efficiency 2D gated X-ray detector, which still needs to be developed.

ACKNOWLEDGMENTS

This work was supported in part by the EC Network grant FMRX-CT96-0080 and the Access to large-scale facility grant ERBFMGECT950020, by the Swedish Medical Research Council, Swedish Natural Science Research Council, Swedish Engineering Sciences Research Council, and the Knut and Alice Wallenberg Foundation.

REFERENCES

af Klinteberg, C., Berg, R., Lindquist, C., Andersson-Engels, S. & Svanberg, S. (1995). *SPIE* **2626**, 149.

af Klinteberg, C., Pifferi, A., Andersson-Engels, S., Cubeddu, R. & Svanberg, S. (1999). *In vivo* Absorption Spectrum of Disulphonated Aluminium Phtalocyanine (AlS_2Pc) in Rats using Femtosecond White Light (to be published).

Andersson-Engels, S., Berg, R., Persson, A. & Svanberg, S. (1993). *Opt. Letters* **18**, 1697.

Berg, R., Jarlman, O. & Svanberg, S. (1993). *Appl. Opt.* **32**, 574.

Cubeddu, R., Pifferi, A., Taroni, P., Torricelli, A. & Valentini, G. (1996). *Med. Phys.* **23**, 1625.

Gmür, N.F., Chapman, D., Thomlinson, W., Thompson, A.C., Lavender, W.M., Scalia, K., Malloy, N., Mangano, J. & Jacob, J. (1995). *Rev. Sci. Instr.* **66**, 1357.

Gordon III, C.L., Yin, G.Y., Lemoff, B.E., Bell, P.B. & Barty, C.P. (1995). *Opt. Lett*, **20**, 1056.

Grätz, M., Pifferi, A., Wahlström, C.-G., & Svanberg, S. (1996). *IEEE JSTQE* **2**, 1041.

Grätz, M., Kiernan, L., Herrlin, K., Wahlström, C.-G. & Svanberg, S. (1998) *Appl. Phys. Lett.* **73**, 2899.

Grätz, M. (1998). PhD Dissertation (Lund Institute of Technology).

Herrlin, K., Svahn, G., Olsson, G., Petterson, H., Tillman, C., Persson, A., Wahlström, C.-G. & Svanberg, S. (1993). *Radiology* **189**, 65.

Herrlin, K., Tillman, C., Grätz, M., Olsson, C., Pettersson, H., Svahn, G., Wahlström, C.-G. & Svanberg, S. (1997). *Invest. Radiology* **32**, 306.

Hölzer, G., Förster, E., Grätz, M., Tillman, C. & Svanberg, S. (1997). *J. X-Ray Sci. Techn.* **7**, 50.

Hölzer, G., Andersson, E., Gibbon, P., Förster, E., Grätz, M., Kiernan, L., Sjögren, A. & Svanberg, S. (1999). *J. Phys. E* (in press).

Johansson. J, Berg, R., Pifferi, A., Svanberg, S. & Björn, L.O. (1999). *Photochem. Photobiol.* **69**, 242.

Kmetec, J.D., Gordon III, C.L., Macklin, J.J., Lemoff, B.E. Brown, G.S. & Harris, S.E. (1992). *Phys. Rev. Lett.* **68**, 1527.

https://doi.org/10.1017/S0263034600183302 Published online by Cambridge University Press

Svanberg, K., Andersson, T., Killander, D., Wang, I., Stenram, U., Andersson-Engels, S., Berg, R., Johansson, J. & Svanberg, S. (1994*a*). *British J. of Dermatology* **130**, 743.

Svanberg, S., Larsson, J., Persson, A. & Wahlström, C.-G. (1994*b*). *Physica Scr.* **49**, 187.

Svanberg, S. (1997). *Phys. Scripta* **T72**, 69.

Svanberg, S. (1999). Tissue Diagnostics using Lasers, *Lasers in Medicine*, Chap. 7, G. Pettit and R.W. Waynant (eds), Plenum, N.Y., to appear.

Tillman, C., Persson, A., Wahlström, C.-G., Svanberg, S. & Herrlin, K. (1995). *Appl. Phys.* B**61**, 333.

Tillman, C., Mercer, I., Svanberg, S. & Herrlin, K. (1996). *J. Opt. Soc. Am.* **13**, 209.

Tillman, C., Grafström, G., Jonsson, A.-C., Jönsson, B.-A., Mercer, I., Mattsson, S., Strand, S.-E. & Svanberg, S. (1999). Survival of Mammalian Cells Exposed to Ultrahigh Dose Rates from a Laser-Produced Plasma X-ray Source. *Radiology* **213**, 860.

Tillman, C., Johansson, S.Å., Erlandsson, B., Grätz, M., Hemdal, B., Almén, A., Mattsson, S. & Svanberg, S. (1997). *Nucl. Instr. Meth.* **A394**, 387.

Tillman, C. (1997). PhD Dissertation (Lund Institute of Technology).

Wang, I., Bendsoe, N., Af Klinteberg, C., Enejder, A.M.N., Andersson-Engels, S., Svanberg, S. & Svanberg, K. (1999). Photodynamic Therapy *versus* Cryosurgery of Basal Cell Carcinomas; Results of a Phase III Clinical Trial, to appear.

https://doi.org/10.1017/S0263034600183302 Published online by Cambridge University Press